Published in final edited form as:
Biochemistry. 2008 September 16; 47(37): 9803–9810. doi:10.1021/bi800659x.

Overexpression and functional characterization of the extracellular domain of the human α1 glycine receptor

Zhenyu Liu[1], **Gomathi Ramanoudjame**[3], **Deqian Liu**[4], **Robert Fox**[4], **Vasanthi Jayaraman**[3], **Maria Kurnikova**[2], and **Michael Cascio**[1,5]

[1]Center for Neuroscience, University of Pittsburgh, Pittsburgh, PA 15261

[2]Department of Chemistry, Carnegie Mellon University, Pittsburgh, PA 15213

[3]Department of Integrative Biology and Pharmacology, University of Texas Health Science Center, Houston, Texas 77030

[4]Department of Biochemistry and Molecular Biology, and The Sealy Center for Structural Biology and Molecular Biophysics, The University of Texas Medical Branch, Galveston, Texas 77555-0647

[5]Department of Molecular Genetics and Biochemistry, University of Pittsburgh School of Medicine, Pittsburgh, Pennsylvania 15261

Abstract

A novel truncated form (residues 1–214, with a randomized C-terminal tail) of the ligand-binding extracellular domain (ECD) of the human α1 glycine receptor (GlyR), with amino acids from the corresponding sequence of an acetylcholine binding protein (AChBP) substituted for two relatively hydrophobic membrane-proximal loops, was overexpressed using a baculovirus expression system. The mutant GlyR ECD, named GlyBP, was present in both soluble and membrane-associated fractions after cell lysis, though only the latter appeared to be in a native-like conformation capable of binding strychnine, a GlyR specific antagonist. The membrane-associated GlyBP was solubilized and detergent/lipid/protein micelles were affinity purified. After detergent removal, GlyBP may be isolated in either aqueous or vesicular form. Binding assays and spectroscopic studies using circular dichroism and FRET are consistent with both forms adopting equivalent native-like conformations. Thus GlyBP may be isolated as a soluble or membrane-associated assembly that serves as a structural and functional homolog of the ECD of GlyR.

The glycine receptor (GlyR) belongs to the Cys-loop family of ligand gated ion channels that includes nicotinic acetylcholine receptors (nAChRs), $GABA_A$ receptors and $5\text{-}HT_3$ receptors (1). These receptors mediate rapid synaptic transmission in the nervous system. Each subunit of this superfamily of pentameric receptors has a large N-terminal extracellular domain (ECD), four membrane-spanning segments that comprise the transmembrane pore domain, and an evolutionarily conserved gating mechanism (2). The ECD contains the eponymous conserved Cys loop as well as sites for agonist and antagonist binding. Proper functioning of the ECD is essential for converting external chemical signals into an altered potential across the plasma membrane, as allosteric changes effected by agonist binding result in transient opening of the channel (gating).

The acetylcholine binding proteins (AChBPs) are secreted soluble proteins that are structural homologs of the ECD of the Cys-loop receptors (3–5). Thus, the crystal structures of various

To whom correspondence should be addressed: M. Cascio (E-mail: cascio@pitt.edu); Phone: (412) 648 - 9488; Fax: (412) 383 - 7220..

Competing interests statement: The authors declare no competing financial interests.

AChBPs in complex with agonists or competitive antagonists (4,6–9) are consistent with the biochemistry of the intersubunit ligand binding sites of full-length receptors (4,10,11). While these crystal structures provide appropriate templates for modeling of the ligand binding domains of Cys-loop receptor family and have greatly advanced our understanding of these domains (5,12,13), the allosteric changes effected upon ligand-binding are less well-characterized and would be expected to be critically dependent of the fine structure at the subunit interfaces, which are less well-conserved between the full-length receptors and AChBPs.

The structure of *Torpedo* nicotinic acetylcholine receptor (nAChR) has been resolved at 4 Å resolution by cryoelectron microscopy (14). However, the molecular mechanisms that define channel gating and subsequent desensitization of this and other Cys-loop receptors remain controversial. Due to difficulties in overexpressing and conducting high resolution structural studies on polytopic, integral membrane proteins, overexpression of a soluble ECD of Cys-loop receptor is an attractive alternative approach as structural studies on this ECD may provide the requisite molecular details essential in understanding how the energy of ligand-binding is used to gate the channel. A number of ECDs of nAChR subunits have been heterologously expressed and characterized (15,16). These ECDs are monomers (16–18) or high-order aggregates (19,20). Recently, a crystal structure of the mouse nAChR α1 ECD bound to alpha-bungarotoxin was determined at 1.94 A resolution (21). This monomeric structure displayed a similar overall fold to that of AChBP, however, few inferences regarding ligand binding and allostery may be learned in the absence of a native-like subunit interface. In addition, The structure of a prokaryotic homolog of the pentameric ligand gated ion channels was resolved very recently, which provided the first pentameric ion channel at high resolution (22).

In this study we have focused on the ECD of GlyR. In adult synapses, a mixture of α and β subunits comprise the functional form of GlyR (23). However, expression of α subunits in heterologous systems yield functional homopentamers that retain the pharmacological properties of native receptors (24,25). Here, we report overexpression, purification and functional characterization of GlyBP, a chimeric protein containing the truncated ECD of α1 GlyR with two substituted hydrophilic loops from AChBP. GlyBP was isolated and characterized in both soluble and vesicle-associated forms.

MATERIALS AND METHODS

Expression of GlyBP in insect cells

To produce a soluble GlyR ECD, the putative hydrophobic loops (resides 144–147 and 182–186 in our pFastBac vector encoding human α1 GlyR, residues 1–214 with a randomized 30 amino acid tail) in the ECD of GlyR were replaced with the corresponding hydrophilic loops of AChBP by a two-step PCR amplification. All constructs were verified by DNA sequencing. The resulting transfer vector, pFastBacGlyBP, was transformed into DH10BAC competent cells for transposition into bacmid. Sf9 cells were then transfected with bacmid encoding GlyBP to generate baculovirus encoding GlyBP following standard protocols. *Spodoptera frugiperda* (Sf9) cells were grown in Grace's Insect Medium supplemented with 10% fetal bovine serum (FBS) and 100 U/ml penicillin/100 μg/ml streptomycin at 28 °C as suspension cultures in spinner flasks under constant rotation (120 rpm). Sf9 cells were infected with virus encoding GlyBP at MOI > 5 and harvested 4 days post-infection.

GlyBP Purification

Harvested Sf9 cells were gently pelleted by centrifugation at 1000 × g for 10 min. Cells were washed three times with ice-cold PBS and resuspended on ice for 1 h in hypotonic solution (5 mM Tris (pH 8.0), 5 mM EDTA, 5 mM EGTA, 10 mM dithiothreitol, and an anti-proteolytic

cocktail containing 1.6 μu/ml aprotinin, 100 μM phenylmethylsulfonyl fluoride, 1 mM bezanmidine and 100μM Benzethonium chloride). Cells (jacketed in an ice bath) were lysed by probe sonication using a microtip (8 × 15 sec, using a 50% cycle). Disrupted cells were centrifuged at 100,000 g for 1 h. Pellets were resuspended at 4 °C overnight in solubilization buffer (25 mM KPi (pH 7.4), 1% digitonin, 0.1% deoxycholate, 0.5 mg/ml Egg PC, 500 mM KCl, 5 mM EDTA, 5 mM EGTA, 10 mM dithiothreitol, and our anti-proteolytic cocktail). Samples were then centrifuged at 100,000 × g and the solubilized supernatant added to 2-aminostrychnine agarose matrix at 4 °C overnight with gentle agitation. The agarose was washed three times with excess wash buffer (solubilization buffer with digitonin reduced to 0.1%), and then eluted for 2 days with solubilization buffer containing 1.5 mM 2-aminostrychnine. The eluate was dialyzed against 100 mM KCl/25 mM KPi (pH 7.4) for 2 h, 20 mM KCl/25 mM KPi (pH 7.4) for another 2 h and then dialyzed against 25 mM KPi (pH 7.4) overnight. After centrifugation at 100,000 × g, the pellet (membrane associated form) was resuspended in 25 mM KPi buffer with a final protein-lipid ratio of ~1: 200 (mol: mol) and the supernatant (aqueous form) was concentrated in an Amicon Ultra-4 centrifugal filter device with a 10 KDa cutoff. Protein concentrations were determined by modified Lowry assay (26). For SDS-PAGE, protein samples were treated with SDS-PAGE sample buffer containing 2 % SDS and heated for 5 min at 95 °C. Proteins were separated by 10% SDS-PAGE and transferred to nitrocellulose. Western immunoblots were developed with monoclonal anti-mouse antibodies against GlyR and horseradish peroxidase (HRP)-conjugated secondary antibody using standard protocols.

Ligand binding assays

For saturation binding assay, purified GlyBP in either aqueous or membrane-associated form were incubated with [^{3}H] strychnine at various concentrations on ice for 30 min in the presence and absence of excess cold strychnine. After precipitation by 15 % PEG400 or PEG6000, the proteins were applied to GF/A filters and washed thoroughly with binding buffer. Radioactivity was determined by liquid scintillation spectrometry. For competitive binding assay, purified GlyBP in the presence of 100 nM of [^{3}H] strychnine was incubated overnight with various concentrations of glycine overnight and binding was quantified as described above. The IC_{50} and B_{max}values were determined using the software GraphPad Prism 3.0. The K_i was calculated using:

$$K_i = IC_{50} / (1 + [\text{radioligand}] / K_d) \quad (27)$$

Circular dichroism (CD)

CD spectra were recorded on an AVIV Model 202 spectrophotometer. CD spectra of aqueous and vesicular forms of GlyBP in 25 mM potassium phosphate buffer, pH 7.4, were all collected at a protein concentration of 0.16 - 0.2 mg/ml at 25 °C in the near-UV length region (190–280 nm). At least ten reproducible spectra were collected for each preparation, averaged, and smoothed (28). All reported spectra were baseline corrected by subtraction of similarly collected, averaged, and smoothed baselines of appropriate buffer, ligands and/or vesicles identically prepared, except without purified protein. Samples containing lipid vesicles were probe sonicated to minimize optical artifacts due to differential light scattering and protein to lipid ratios were minimized low to ensure negligible absorption flattening effects. The CD spectra of the protein in the near UV region were analyzed using DICHROWEB (29,30) (public-1.cryst.bbk.ac.uk/cdweb/html/). Spectra were analyzed using CDSSTR (31), or CONTINLL (32) and a normalized root mean standard deviation (NRMSD) value was calculated as a measure of the fit of the calculated curve to the experimental data (33).

Dynamic light scattering

Purified GlyBP, in 25 mM KPi (pH 7.4) and 1 mM DTT was diluted to a final monomer protein concentration of 0.4 mg/mL. Samples were filtered with a 0.22 um Millipore Millex-GV filter and analyzed in a Wyatt Protein Solutions DynaPro instrument. Dynamic light scattering data were collected in triplicate and analyzed with the Protein Solutions DynaPro software.

Förster Resonance Energy Transfer (FRET)

1 μM purified GlyBP in 25 mM KPi (pH 7.4) with 100 μM glycine (Sigma-Aldrich) was labeled with a 1:4 ratio of the maleimide derivatives of fluorescein (Biotium, Hayward, CA) and triethylenetetraminehexaacetic acid chelate of terbium (TTHA-Tb) (Invitrogen) for the donor:acceptor sample and with terbium chelate alone for the donor-only sample. Protein was dialyzed in phosphate buffered saline.

For FRET studies on full-length GlyRs, Sf9 cells were infected with either wild-type baculovirus (no GlyR) or with baculovirus encoding full-length GlyR. Cells were pre-labeled by treatment with 10 mM iodoacetamide for 1 h at 28 °C at 6 h post-infection to block endogenous free thiol groups on the cell surface. Cells were collected by gentle centrifuguation at 1000 × g, washed twice with serum-free medium and then resuspended in FBS-containing medium and allowed to grow at 28 °C. Thus, only accessible extracellular Cys residues of those membrane proteins expressed on the surface after this time are available for labeling. Cells were collected by gentle centrifugation at 1000 × g, washed with extracellular buffer and labeled with the 1:4 ratio of fluorescein and terbium chelate for 90 min. Cells were then washed with extracellular buffer for fluorescence lifetime measurements.

A TimeMaster Model TM-3M /2003 (Photon Technology International, Lawrenceville, NJ) was used for spectroscopic measurements. A nitrogen/dye laser system was fiber-optically coupled to the sample compartment containing a thermostable cuvette holder with a microstirrer. Emitted light was collected by quartz optics and passed through a monochromator to a stroboscopic detector. Data were collected using Felix software (Photon Technologies International, Lawrenceville, NJ) and analyzed using Origin (OriginLab, Northampton, MA). Calculated lifetimes are an average of at least two different data sets and for each set the data were an average of five shots. Using the time constants of the donor fluorescence decay (τ_D) and the sensitized emission of the acceptor due to energy transfer from donor (τ_{DA}), the distances between the donor and acceptor are calculated by Förster's theory of energy transfer, with:

$$R = R_o \left(\frac{\tau_{DA}}{\tau_D - \tau_{DA}} \right)^{1/6}$$

R_o was calculated using overlap integral as described previously (34,35).

RESULTS

Construction and overexpression of GlyBP in Sf9 insect cells

In our hands, extensive attempts to overexpress the ECD of the α1 subunit of GlyR, either as a truncated protein or fusion protein in a variety of expression systems, failed to produce soluble native-like oligomers capable of binding strychnine (unpublished observations). Given that AChBP is a secreted pentameric homolog of the ECD of Cys-loop receptors, we hypothesized that the ECD of GlyR might be expressed as a native-like soluble complex if the relatively hydrophobic membrane-proximal loops in the ECD of the full-length receptor (loops 7 and 9)

were replaced with their relatively hydrophilic counterparts in AChBP (Figure 1; for full sequence see Figure 1S). This protein, designated glycine binding protein (GlyBP), was expressed in a baculoviral expression system and GlyBP expression appeared to reach its highest level four days after infection (Figure 2S). GlyBP was detected in both cytosolic and membrane-associated fractions in Western immunoblots of fractionated cells (Figure 2A). Membrane-associated GlyBP in the pelleted lysate was solubilized by incubation with digitonin/deoxylcholate using conditions identical to that used to solubilize full-length GlyR in native form (24,36). The membrane-associated fraction, but not the cytosolic fraction, bound to the 2-aminostrychnine affinity resin (Figure 2B and C), suggesting that only membrane-associated GlyBP adopts a native-like structure. Hence, only membrane-associated GlyBP was subsequently characterized. Thus, despite replacing loops 7 and 9 of the GlyR ECD with the more hydrophilic sequences from AChBP, GlyBP still partitions with membranes even though the truncated protein lacks hydrophobic transmembrane segments. Other investigators also observed that a refolded form of the ECD of GlyR expressed in bacteria was strongly membrane-associated (37).

Purification of GlyBP

GlyBP/detergent/lipid micelles were bound to a 2-aminostrychnine affinity resin, and > 90% of bound GlyBP could be eluted with 1.5 mM 2-aminostrychnine (Figure 2D). The predominant matching bands on Western Imunoblots and stained SDS-PAGE gels (Figure 2F) show purified GlyBP runs as a doublet. Despite reduction and denaturation, some immunoreactive higher order bands are observed. A similar phenomenon was also observed in full-length α1 GlyR which is also observed as a doublet on SDS-PAGE and is visualized as higher order aggreagates (36, 38). This anamalous migration of GlyBP might be due to: 1) heterogeneity in the unfolding of GlyBP and/or differential binding of SDS such that two predominant species with altered shape and/or charge distribution of the monomeric protein are present giving rise to anomalous migration; or 2) differential post-translational modifications of GlyBP in insect cells; or 3) partial proteolysis of the protein *in vivo* or during sample preparation. Given that the most common post-translational modification consistent with large mass shifts are glycosylations, both forms of GlyBP were incubated with deglycosidases Endo H or PNGases. In neither case was any significant molecular mass shift observed using SDS-PAGE (data not shown), indicating that the doublet is probably not due to the presence of differential glycosylation. While we cannot rule out partial proteolysis or clipping, subsequent characterization of GlyBP, as well as its binding to the strychnine resin during purification, suggests that this event, if it occurs, does not result in misfolding of GlyBP as it continues to bind agonist and antagonist. In addition, mass fingerprinting of both bands of the analogous doublet in SDS-PAGE of full-length GlyR gave coverage over the entire primary sequence of GlyR, suggesting that the doublet, in this case, is not due to any proteolytic degradation at either the amino- or carboxy-termini of the full-length receptor (Tillman and Cascio, unpublished observation). We propose that the observed GlyBP doublet is most likely due to anomalous migration of GlyBP. In addition, in all cases where observed bands were subjected to mass fingerprinting, no proteins other than GlyBP were identified (unpublished observation). Overall, the high affinity binding of GlyBP to the aminostrychnine matrix allows us to rigorously extract other proteins and provides highly purified protein for subsequent characterization.

Purified GlyBP/detergent/lipid micelles were then dialyzed to remove detergent and salt, yielding protein and vesicles in buffered solution. After brief probe sonication to produce small and unilamellar vesicles, vesicles were pelleted by ultracentrifugation. GlyBP was found at approximately equal levels in both the supernatant, as a soluble protein (aqueous form), and with pelleted lipid vesicles (vesicular form)(Figure 2E). Both fractions bind 2-aminostrychnine resin as assayed in rebinding studies (data not shown). Isolation of GlyBP as a soluble protein (without potentially-interfering associated lipids and/or detergents) is especially significant as

this provides an excellent candidate for high-resolution structural studies. Partitioning ratios of GlyBP with vesicles or in solution were variable in our hands, and are expected to vary with salt concentration, lipid composition, and other variables. Both forms of GlyBP were further characterized to determine which (or if both) of these are homologs of the corresponding structure of the ECD in full-length GlyR.

Ligand binding properties of GlyBP

Given the correlation of structure and function, one can assess whether the structure of GlyBP approximates that of the ECD of the full-length receptor by comparing its affinity for agonist and competitive antagonist in functional binding studies to that of published values for homomeric α1 GlyR. The vesicular form of GlyBP has a K_d of 119±28 nM for [^{3}H]strychnine while K_d of the aqueous form of GlyBP is 230±88 nM (Figure 3A and B), indicating that both forms of GlyBPs remain high affinity for its antagonist strychnine although they showed somewhat reduced affinities compared with the 10–30 nM K_d of full-length α1 GlyR homopentamers (39, 40). B_{max} values indicate that the mole ratio of strychnine bound per mole of GlyBP is 0.88 ± 0.14 and 0.81 ± 0.16 for vesicular and aqueous forms of GlyBP, respectively, so most, if not all, purified protein retains ability to bind to strychnine. Glycine binding assays were conducted by measuring displacement of bound [^{3}H]strychnine and the calculated K_i values are 90.3 ± 16.0 μM for the vesicular form and 71.8 ± 15.4 μM for the aqueous form (Figure 3C and D), which is in general agreement with reported K_i of 20–60 μM for full length pentameric α1 GlyR (41–43). Thus both forms of GlyBP retain native-like affinities for their cognate ligands.

Secondary structure of GlyBP

CD spectroscopy in the low-UV region (190–240 nm) is a particularly useful tool to compare the net secondary structure of proteins since the peptide transitions that give rise to the diagnostic net spectrum in this region are sensitive to small changes in backbone conformation. Given the achiral nature of the vesicle lipids, one may directly compare the net spectra of the aqueous and vesicle associated forms of GlyBP, providing the lipid-protein ratio is sufficiently high and that the vesicles are small and unilamellar in order to minimize absorption flattening effects and differential scattering, respectively (44). Purified GlyBP in either its aqueous soluble form or associated with small unilamellar vesicles were examined in comparative CD studies. The resulting CD spectra of purified GlyBP in either form are nearly superimposable (Figure 4), strongly suggesting their conformations are essentially equivalent whether in solution or associated with vesicles.

Historically, the capability of CD to accurately determine the secondary structure of proteins with reduced helical content, has been limited by the poor representation of some non-helical folds in the reference databases, the reduced signal of α-structures relative to that from helical components, and the structural variability of non-helical folds that gives rise to spectral diversity (45). This has been redressed by the recent generation of a new reference database that more effectively covers secondary structure and fold space (46). Spectra were analyzed by two independent methods using this new database. Both forms of GlyBP had very little helical content and were enriched in α-structure (Table 1), consistent with a net secondary structure homologous to that of AChBP (3,5) and consistent with the reduced helical content determined in CD studies of full-length GlyR reconstituted in vesicles (24). In all analyses the NRMSD value was ≤ 0.05, indicating that the reference data set is appropriate (a value below 0.10 indicate a reasonably good fit of the calculated and experimental spectra; other reference databases gave NRMSD values that were typically above 0.2).

Confirmation of GlyBP oligomeric state by dynamic light scattering

Dynamic light scattering studies were conducted to confirm the oligomeric nature of the soluble form of GlyBP (the presence of vesicles precludes conducting parallel studies on the membrane-associated form). Purified GlyBP has a bimodal polydisperse distribution in these light scattering studies. A small quantity of large aggregates had an R_h ~20 nm. The predominant species were present in a peak with a corresponding R_h of 5.63 +/− 0.05 nm, with moderate polydispersity. Thess values are consistent with a pentameric form of GlyBP with moderate association of pentamers. The polydispersity of the 5.63 nm peaks makes a specific estimate of the molecular weight unreliable; however, the dynamic light scattering study indicates that the soluble form of GlyBP *in vitro* has a globular structure whose dimensions are consistent with those expected for a homopentamer having homology with the ECD of GlyR.

Examination of GlyBP structure by FRET

Förster resonance energy transfer (FRET) has been widely used to measure distances between molecules or conformational changes within an individual molecule as the excited-state energy of a fluorophore may be transferred non-radiatively to a ground-state acceptor fluorophore by long-range (10 –100Å) resonance coupling between the donor and acceptor transition dipoles. The sole free thiol group in GlyBP at Cys41 was reacted with donor or donor:acceptor fluorophores and the FRET efficiency was used to determine the distances between subunits of vesicular GlyBP. The fluorescence lifetime for the protein tagged with donor only (terbium chelate labeled) can be well represented by a single exponential decay (Figure 3S A) and the lifetimes are similar in the absence and presence of glycine (Table 2). The FRET lifetime for the donor:acceptor tagged protein required two exponentials (Figure 5A and SI Figure 4S for single exponential fit), and the FRET lifetime in the presence of glycine is slightly shorter than in the apo state (Table 2). The derived intersubunit distances between Cys-41 are 33.8 and 46.2 Å in the absence of glycine and 31.9 and 44.4 Å in the presence of glycine. Additionally, addition of glycine decreased the distances slightly between inter-subunit Cys-41, indicating glycine-binding induces conformational changes in GlyBP.

To further confirm that GlyBP is a functional homolog of the ECD of GlyR, FRET studies analogous to those conducted on GlyBP were conducted on full-length α1 GlyR expressed on the surface of baculovirus-infected Sf9 cells and the inter-subunit distances between labels on Cys-41 were measured (control studies of non-transfected and transfected cells are shown in Figure 5S). While the full-length receptor contains three unpaired Cys residues, only Cys-41 is accessible to thiol-reactive compounds externally applied in the absence of ligand. Similar to studies on GlyBP, the fluorescence lifetime for the protein tagged with donor only could be well represented by a single exponential decay (Figure 3S B), while the FRET lifetime for the donor:acceptor tagged protein required two exponentials (Figure 5B and Table 2) and the intersubunit distances between Cys-41 are 33.1 and 45.2 Å in the absence of glycine. The calculated distances are reduced to 31.9 and 43.8 Å in the presence of glycine. The distances for the apo and glycine bound states are similar to the distances between Cys-41 in GlyBP, and move closer in the presence of agonist. These studies suggest that GlyBP and GlyR have similar structures and most likely undergo similar allosteric changes upon binding glycine.

DISCUSSION

The determinations of crystal structures of AChBPs have provided useful structural information regarding to the homologous ligand-binding ECDs of Cys-loop receptors. However, the dynamic nature of receptor allostery is dependent on conformational changes induced by ligand binding. Studies based upon the crystal structures of homologous AChBPs, a, while offering a wonderful structural template that provides invaluable insight into molecular

recognition by nAChRs, may not necessarily be a good functional template for understanding ligand-binding dynamics in full length Cys-loop receptors (47,48). Thus, it is necessary to conduct direct structural studies on the entire receptor or on isolated domains that have been shown to be native-like in structure and function. In the last decade, a handful of extracellular domains of Cys-loop receptor family have been overexpressed using various expression systems (16,17,37,49), but a soluble native-like penatmeric form of the ECD had not been previously characterized.

In insect cells, overexpressed GlyBP is present in both cytosolic and membrane fractions after subcellular fractionation. Based on affinity to the stychnine-based chromatographic matrix, somewhat surprisingly, the cytosolic GlyBP appears to be non-native, while the membrane-associated protein seemingly adopts a native-like conformation. This suggests that correct folding of GlyBP may be dependent on the presence of a high local concentration of vectorially-oriented samples on a membrane surface. The association of expressed GlyBP with the membranes of insect cells suggests that additional sequences other than loop 7 and loop 9, the putative membrane-proximal loops of the ECD of GlyR that were replaced by more hydrophilic sequences in this study, are involved in correct association and orientation of this domain at the membrane surface. Patches of negative charges on the surface of GlyBP may form favorable ionic interactions with cationic lipid headgroups that enrich the extracellular leaflet of the plasma membrane. Further mutagenesis studies on other regions of the ECD of GlyR may allow us to better understand how the extracellular domain interacts with the membrane bilayer and how signals transit from the outside of the cell membrane (i.e., external ligand binding sites) to the pore (i.e., the gate(s) of the channel) upon ligand binding.

Quantitation of dissociation constants and ligand/receptor stoichiometry supports the hypothesis that the quaternary structure of the ECD is in a native-like conformation. *In toto*, the experimental studies indicate that both forms of GlyBP adopt similar, native-like three-dimensional structures and either of them could be a potential *structural* homolog of the ECD of GlyR (and, by homology, the ECD of any Cys-loop receptor). Significantly, FRET studies comparing changes in the inter-subunit distances of labeled C41 residues upon glycine binding suggest that in both the full-length receptor in live Sf9 cells and the purified GlyBP associated with vesicles, the protein undergoes similar small, but reproducible allosteric changes upon glycine binding (Table 2). This suggests that GlyBP may be a appropriate *functional* homolog of the ECD of GlyR. Although a large number of soluble, ECDs of distinct subunits of AChRs or GlyR have been overexpressed (16–18,37), this report describes the first time that a native-like pentameric ECD of any Cys-loop receptor has been overexpressed, purified, and characterized. It is hoped that further studies on this protein will provide more insight on our understanding of the complex, pentameric Cys-loop receptor family of ligand-gated ion channels.

Tommy Tillman is thanked for comments, discussions, and suggestions during preparation of this manuscript.

Supplementary Material

Refer to Web version on PubMed Central for supplementary material.

Acknowledgments

This work was partially supported by NIH grants GM51911 (M.C.), DA016381 (M.C.), GM055851 (R.O.F.), GM073102 (V.J.), and GM067962-01 (M.K.), and a Welch Foundation grant (H-1345) (R.O.F.). We also acknowledge the NIH Shared Instrumentation Grant 1S10RR11998 which provided support for the circular dichrometer

Abbreviations

GlyR, glycine receptor; GlyBP, glycine binding protein; AChBP, acetylcholine binding protein; nAChRs, nicotinic acetylcholine receptors; ECD, extracellular domain; CD, circular dichroism; FRET, Förster resonance energy transfer; TTHA-Tb, triethylenetetraminehexaacetic acid chelate of terbium.

References

1. Karlin A, Akabas MH. Toward a structural basis for the function of nicotinic acetylcholine receptors and their cousins. Neuron 1995;15:1231–1244. [PubMed: 8845149]
2. Tasneem A, Iyer L, Jakobsson E, Aravind L. Identification of the prokaryotic ligand-gated ion channels and their implications for the mechanisms and origins of animal Cys-loop ion channels. Genome Biology 2005;6:R4. [PubMed: 15642096]
3. Brejc K, van Dijk WJ, Klaassen RV, Schuurmans M, van Der Oost J, Smit AB, Sixma TK. Crystal structure of an ACh-binding protein reveals the ligand-binding domain of nicotinic receptors. Nature 2001;411:269–276. [PubMed: 11357122]
4. Smit AB, Celie PH, Kasheverov IE, Mordvintsev DY, van Nierop P, Bertrand D, Tsetlin V, Sixma TK. Acetylcholine-binding proteins: functional and structural homologs of nicotinic acetylcholine receptors. J Mol Neurosci 2006;30:9–10. [PubMed: 17192605]
5. Sixma TK, Smit AB. Acetylcholine binding protein (AChBP): a secreted glial protein that provides a high-resolution model for the extracellular domain of pentameric ligand-gated ion channels. Annu Rev Biophys Biomol Struct 2003;32:311–334. [PubMed: 12695308]
6. Celie PH, Kasheverov IE, Mordvintsev DY, Hogg RC, van Nierop P, van Elk R, van Rossum-Fikkert SE, Zhmak MN, Bertrand D, Tsetlin V, Sixma TK, Smit AB. Crystal structure of nicotinic acetylcholine receptor homolog AChBP in complex with an alpha-conotoxin PnIA variant. Nat Struct Mol Biol 2005;12:582–588. [PubMed: 15951818]
7. Celie PH, Klaassen RV, van Rossum-Fikkert SE, van Elk R, van Nierop P, Smit AB, Sixma TK. Crystal structure of acetylcholine-binding protein from Bulinus truncatus reveals the conserved structural scaffold and sites of variation in nicotinic acetylcholine receptors. J Biol Chem 2005;280:26457–26466. [PubMed: 15899893]
8. Celie PH, van Rossum-Fikkert SE, van Dijk WJ, Brejc K, Smit AB, Sixma TK. Nicotine and carbamylcholine binding to nicotinic acetylcholine receptors as studied in AChBP crystal structures. Neuron 2004;41:907–914. [PubMed: 15046723]
9. Hansen SB, Sulzenbacher G, Huxford T, Marchot P, Taylor P, Bourne Y. Structures of Aplysia AChBP complexes with nicotinic agonists and antagonists reveal distinctive binding interfaces and conformations. Embo J 2005;24:3635–3646. [PubMed: 16193063]
10. Corringer PJ, Le Novere N, Changeux JP. Nicotinic receptors at the amino acid level. Annu Rev Pharmacol Toxicol 2000;40:431–458. [PubMed: 10836143]
11. Lynch JW. Molecular structure and function of the glycine receptor chloride channel. Physiol Rev 2004;84:1051–1095. [PubMed: 15383648]
12. Grutter T, Prado de Carvalho L, Virginie D, Taly A, Fischer M, Changeux JP. A chimera encoding the fusion of an acetylcholine-binding protein to an ion channel is stabilized in a state close to the desensitized form of ligand-gated ion channels. C R Biol 2005;328:223–234. [PubMed: 15810546]
13. Brejc K, van Dijk WJ, Smit AB, Sixma TK. The 2.7 A structure of AChBP, homologue of the ligand-binding domain of the nicotinic acetylcholine receptor. Novartis Found Symp 2002;245:22–29. [PubMed: 12027010]discussion 29–32, 165–168
14. Unwin N. Refined structure of the nicotinic acetylcholine receptor at 4A resolution. J Mol Biol 2005;346:967–989. [PubMed: 15701510]
15. Tierney ML, Unwin N. Electron microscopic evidence for the assembly of soluble pentameric extracellular domains of the nicotinic acetylcholine receptor. J Mol Biol 2000;303:185–196. [PubMed: 11023785]

16. Yao Y, Wang J, Viroonchatapan N, Samson A, Chill J, Rothe E, Anglister J, Wang ZZ. Yeast expression and NMR analysis of the extracellular domain of muscle nicotinic acetylcholine receptor alpha subunit. J Biol Chem 2002;277:12613–12621. [PubMed: 11812776]
17. West AP Jr, Bjorkman PJ, Dougherty DA, Lester HA. Expression and circular dichroism studies of the extracellular domain of the alpha subunit of the nicotinic acetylcholine receptor. J Biol Chem 1997;272:25468–25473. [PubMed: 9325259]
18. Psaridi-Linardaki L, Mamalaki A, Remoundos M, Tzartos SJ. Expression of soluble ligand- and antibody-binding extracellular domain of human muscle acetylcholine receptor alpha subunit in yeast Pichia pastoris. Role of glycosylation in alpha-bungarotoxin binding. J Biol Chem 2002;277:26980–26986. [PubMed: 12015305]
19. Tsetlin VI, Dergousova NI, Azeeva EA, Kryukova EV, Kudelina IA, Shibanova ED, Kasheverov IE, Methfessel C. Refolding of the Escherichia coli expressed extracellular domain of alpha 7 nicotinic acetylcholine receptor. Eur J Biochem 2002;269:2801–2809. [PubMed: 12047391]
20. Avramopoulou V, Mamalaki A, Tzartos SJ. Soluble, oligomeric, and ligand-binding extracellular domain of the human alpha7 acetylcholine receptor expressed in yeast: replacement of the hydrophobic cysteine loop by the hydrophilic loop of the ACh-binding protein enhances protein solubility. J Biol Chem 2004;279:38287–38293. [PubMed: 15226316]
21. Dellisanti CD, Yao Y, Stroud JC, Wang Z-Z, Chen L. Crystal structure of the extracellular domain of nAChR [alpha]1 bound to [alpha]-bungarotoxin at 1.94 A resolution. Nat Neurosci 2007;10:953–962. [PubMed: 17643119]
22. Hilf RJC, Dutzler R. X-ray structure of a prokaryotic pentameric ligand-gated ion channel. Nature 2008;452:375–379. [PubMed: 18322461]
23. Grudzinska J, Schemm R, Haeger S, Nicke A, Schmalzing G, Betz H, Laube B. The beta subunit determines the ligand binding properties of synaptic glycine receptors. Neuron 2005;45:727–739. [PubMed: 15748848]
24. Cascio M, Shenkel S, Grodzicki RL, Sigworth FJ, Fox RO. Functional reconstitution and characterization of recombinant human alpha 1-glycine receptors. J Biol Chem 2001;276:20981–20988. [PubMed: 11145968]
25. Bormann J, Rundstrom N, Betz H, Langosch D. Residues within transmembrane segment M2 determine chloride conductance of glycine receptor homo- and hetero-oligomers. Embo J 1993;12:3729–3737. [PubMed: 8404844]
26. Peterson GL. A simplification of the protein assay method of Lowry et al. which is more generally applicable. Anal Biochem 1977;83:346–356. [PubMed: 603028]
27. Cheng Y, Prusoff WH. Relationship between the inhibition constant (K1) and the concentration of inhibitor which causes 50 per cent inhibition (I50) of an enzymatic reaction. Biochem Pharmacol 1973;22:3099–3108. [PubMed: 4202581]
28. Savitzky A, Golay MJE. Smoothing and Differentiation of data by a simplified least squares procedures. Anal. Chem 1964;36:1627–1639.
29. Lobley A, Whitmore L, Wallace BA. DICHROWEB: an interactive website for the analysis of protein secondary structure from circular dichroism spectra. Bioinformatics 2002;18:211–212. [PubMed: 11836237]
30. Whitmore L, Wallace BA. DICHROWEB, an online server for protein secondary structure analyses from circular dichroism spectroscopic data. Nucleic Acids Res 2004;32:W668–W673. [PubMed: 15215473]
31. Sreerama N, Woody RW. Estimation of protein secondary structure from circular dichroism spectra: comparison of CONTIN, SELCON, and CDSSTR methods with an expanded reference set. Anal Biochem 2000;287:252–260. [PubMed: 11112271]
32. Provencher SW, Glockner J. Estimation of globular protein secondary structure from circular dichroism. Biochemistry 1981;20:33–37. [PubMed: 7470476]
33. Mao D, Wachter E, Wallace BA. Folding of the mitochondrial proton adenosinetriphosphatase proteolipid channel in phospholipid vesicles. Biochemistry 1982;21:4960–4968. [PubMed: 6291595]
34. Du M, Reid SA, Jayaraman V. Conformational changes in the ligand-binding domain of a functional ionotropic glutamate receptor. J Biol Chem 2005;280:8633–8636. [PubMed: 15632199]

35. Ramanoudjame G, Du M, Mankiewicz KA, Jayaraman V. Allosteric mechanism in AMPA receptors: a FRET-based investigation of conformational changes. Proc Natl Acad Sci U S A 2006;103:10473–10478. [PubMed: 16793923]
36. Cascio M, Schoppa NE, Grodzicki RL, Sigworth FJ, Fox RO. Functional expression and purification of a homomeric human alpha 1 glycine receptor in baculovirus-infected insect cells. J Biol Chem 1993;268:22135–22142. [PubMed: 8408073]
37. Breitinger U, Breitinger HG, Bauer F, Fahmy K, Glockenhammer D, Becker CM. Conserved high affinity ligand binding and membrane association in the native and refolded extracellular domain of the human glycine receptor alpha1-subunit. J Biol Chem 2004;279:1627–1636. [PubMed: 14593111]
38. Griffon N, Buttner C, Nicke A, Kuhse J, Schmalzing G, Betz H. Molecular determinants of glycine receptor subunit assembly. Embo J 1999;18:4711–4721. [PubMed: 10469650]
39. Graham D, Pfeiffer F, Simler R, Betz H. Purification and characterization of the glycine receptor of pig spinal cord. Biochemistry 1985;24:990–994. [PubMed: 2581608]
40. Sanes DH, Geary WA, Wooten GF, Rubel EW. Quantitative distribution of the glycine receptor in the auditory brain stem of the gerbil. J Neurosci 1987;7:3793–3802. [PubMed: 2890726]
41. Marvizon JC, Vazquez J, Garcia Calvo M, Mayor F Jr, Ruiz Gomez A, Valdivieso F, Benavides J. The glycine receptor: pharmacological studies and mathematical modeling of the allosteric interaction between the glycine- and strychnine-binding sites. Mol Pharmacol 1986;30:590–597. [PubMed: 3023812]
42. Lynch JW, Rajendra S, Pierce KD, Handford CA, Barry PH, Schofield PR. Identification of intracellular and extracellular domains mediating signal transduction in the inhibitory glycine receptor chloride channel. Embo J 1997;16:110–120. [PubMed: 9009272]
43. Breitinger HG, Villmann C, Becker K, Becker CM. Opposing effects of molecular volume and charge at the hyperekplexia site alpha 1(P250) govern glycine receptor activation and desensitization. J Biol Chem 2001;276:29657–29663. [PubMed: 11395484]
44. Mao D, Wallace BA. Differential light scattering and absorption flattening optical effects are minimal in the circular dichroism spectra of small unilamellar vesicles. Biochemistry 1984;23:2667–2673. [PubMed: 6466606]
45. Wallace BA, Lees JG, Orry AJ, Lobley A, Janes RW. Analyses of circular dichroism spectra of membrane proteins. Protein Sci 2003;12:875–884. [PubMed: 12649445]
46. Lees JG, Miles AJ, Wien F, Wallace BA. A reference database for circular dichroism spectroscopy covering fold and secondary structure space. Bioinformatics 2006;22:1955–1962. [PubMed: 16787970]
47. Dellisanti CD, Yao Y, Stroud JC, Wang ZZ, Chen L. Crystal structure of the extracellular domain of nAChR alpha1 bound to alpha-bungarotoxin at 1.94 A resolution. Nat Neurosci. 2007
48. Karlin A. A touching picture of nicotinic binding. Neuron 2004;41:841–842. [PubMed: 15046715]
49. Fischer M, Corringer P-J, Schott K, Bacher A, Changeux J-P. A method for soluble overexpression of the alpha 7 nicotinic acetylcholine receptor extracellular domain. Proc Natl Acad Sci 2001;98:3567–3570. [PubMed: 11248118]

A

Protein	Sequence
AChBP	C D V S G V *D T E S* G - A T C
α7 nAChR	C Y I D V R W F P F D V Q H C
α1 GlyR	C P M D L K *N F P M* D V Q T C
	138 144 147 152
AChBP	S E Y F *S Q Y S R* F E I L D
α7 nAChR	I S G Y I P N G E W D L V G
α1 GlyR	V A D G *L T L P Q* F I L Q E
	178 182 186 191

B

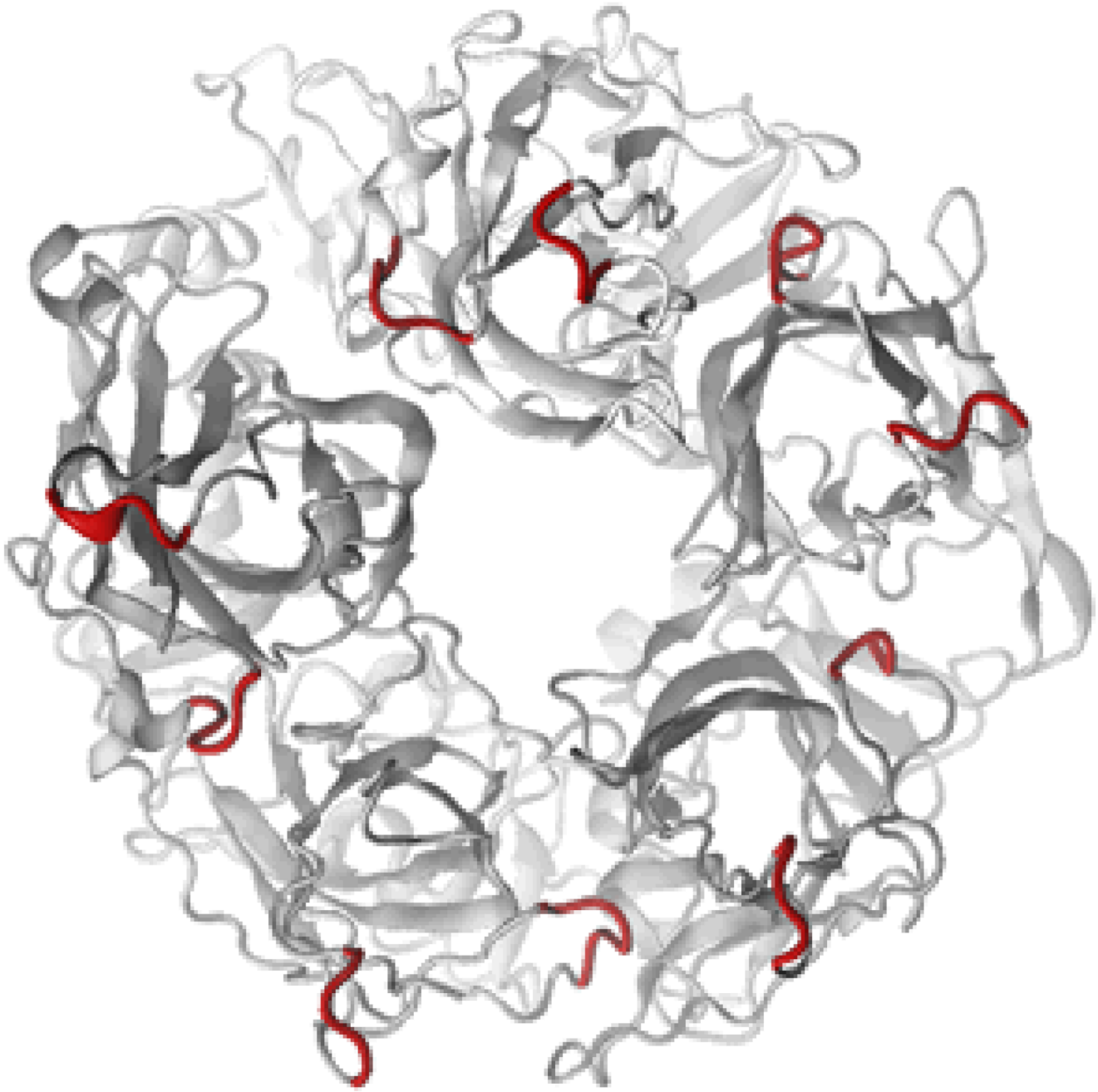

FIGURE 1.

Construction of GlyBP. (A) Partial sequence alignment of *Lymnaea stagnalis* AChBP (GenBank accession #: AAK64377), human α7 nAChR (GenBank accession #: NP_000737) and human α1 GlyR (GenBank accession #: P23415). Shown are Loop 7 and Loop 9 with flanking sequence. Numbering refers to residue numbers for α1 GlyR. Substituted amino acids are highlighted in gray. (B) Schematic diagram showing backbone of GlyBP model with putative membrane-proximal loops facing the viewer. Substituted amino acids are highlighted in red.

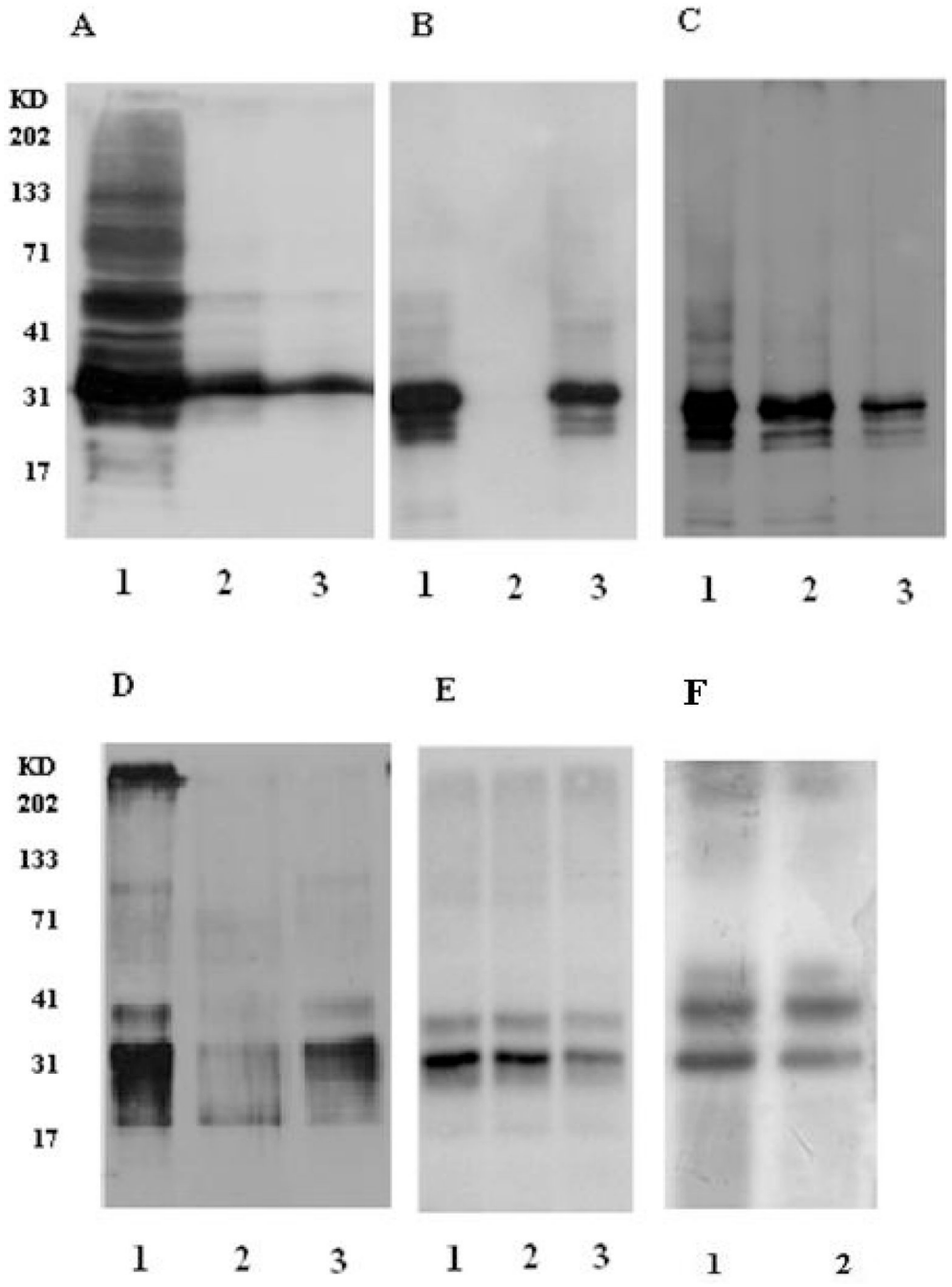

FIGURE 2.

Overexpression of GlyBP in Sf9 insect cells and binding to 2-aminostrychnine (2-AS) affinity matrix. All panels are Western immunoblots except where otherwise noted. (A) Subcellular fractionation of GlyBP. Lane 1 - total extract of Sf9 cells 4 days post-infection, Lane 2 - cytosolic fraction, Lane 3 - membrane-associated pellet. (B) Cytosolic fraction failed to bind to 2-AS resin. Lane1: total cytosolic protein, Lane 2: protein bound to 2-AS resin, Lane 3: unbound protein. (C) Membrane fraction bound to 2-AS resin. Lane 1: total membrane fraction, Lane 2: protein bound to 2-AS resin, Lane 3: unbound protein. (D) Elution of membrane-associated GlyBP from 2-AS resin. Lane 1: GlyBP bound to 2-AS resin, Lane 2: GlyBP bound to 2-AS resin after elution with 1.5 mM 2-AS; Lane 3: protein eluate after incubation with 1.5

mM 2-AS. (E) Partitioning of purified GlyBP after detergent dialysis (Lane 1) and ultracentrifugation (Lanes 2 and 3). Lane 2: aqueous form of GlyBP, Lane 3: vesicular form of GlyBP. (F) Silver staining of purified aqueous (lane 1) and vesicular (lane 2) forms of GlyBP.

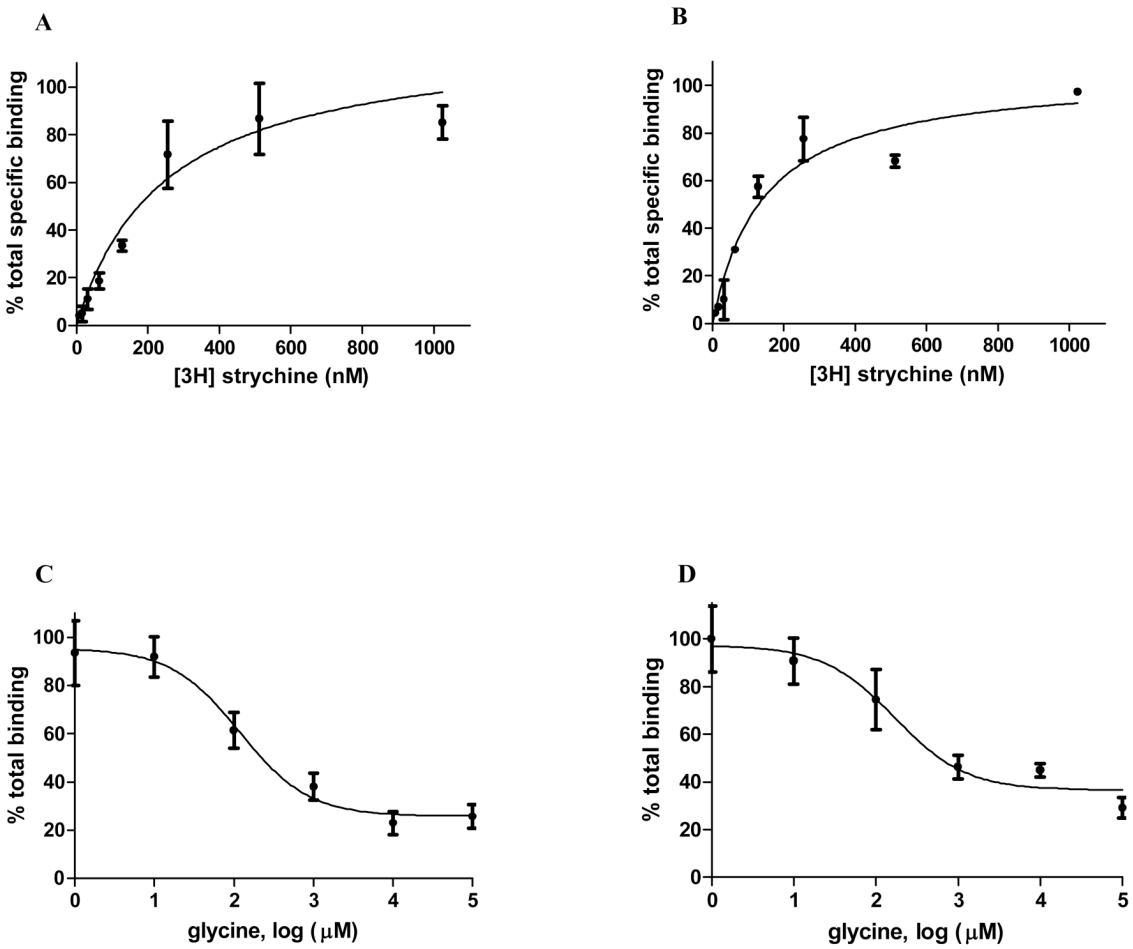

FIGURE 3.

GlyBP binding assays. [^{3}H]Strychnine saturation binding for aqueous (A) and vesicular form (B) of GlyBP. Both forms of purified GlyBP were incubated with various concentrations of [^{3}H]Strychnine in the absence and presence of cold strychnine. After precipitation with 15% PEG400, bound [^{3}H]Strychnine was collected by rapid filtration and radioactivity was determined by liquid scintillation spectrometry. Competitive glycine binding for [^{3}H] strychnine-bound aqueous (C) and vesicular form (D) of GlyBP. Similary, both forms of purified GlyBP were pre-incubated with [^{3}H]Strychnine and then various concentrations of glycine were added to compete with bound [^{3}H]Strychnine. After precipitated with 15% PEG6000, bound [^{3}H]Strychnine was collected by rapid filtration and radioactivity was determined by liquid scintillation spectrometry.

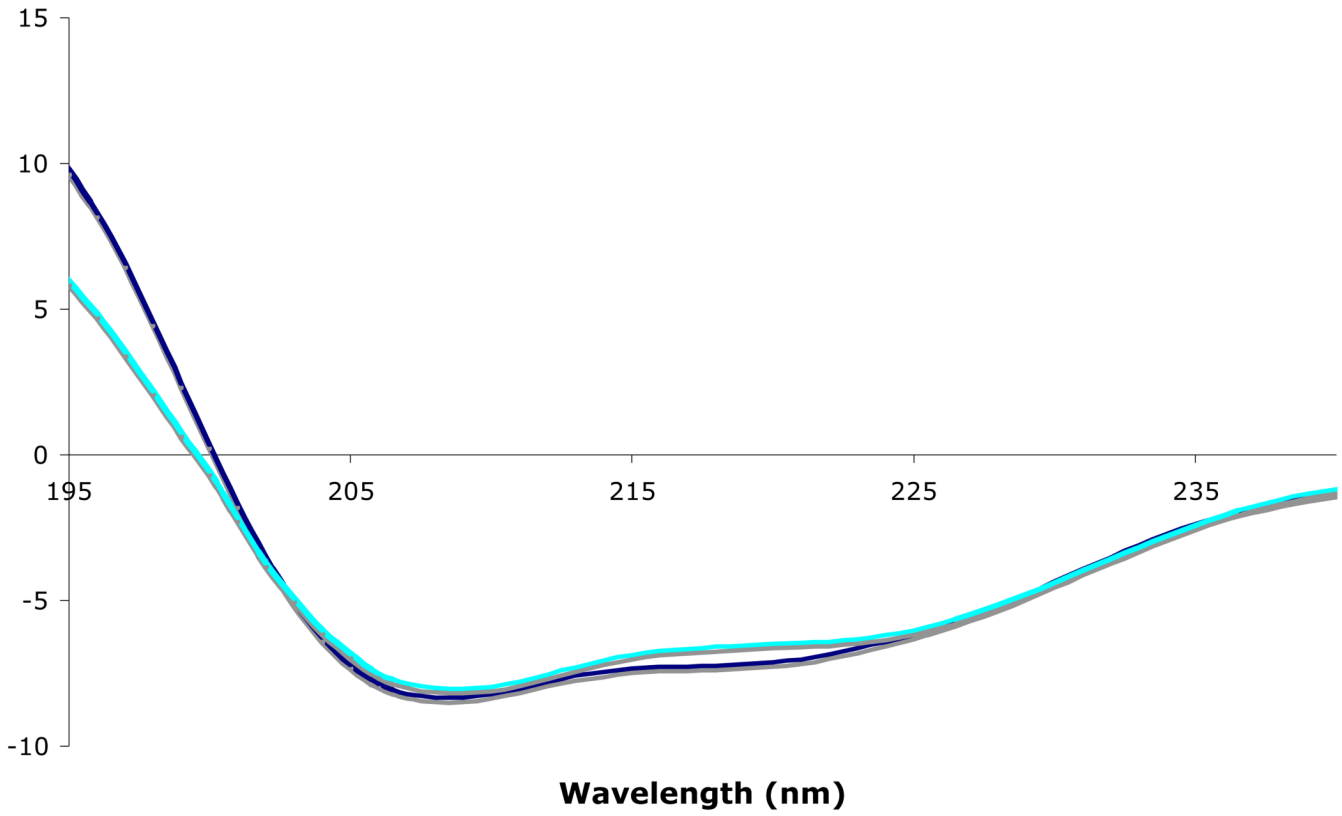

FIGURE 4.

CD spectra of aqueous (blue) and vesicular (cyan) forms of GlyBP. CD spectra of both forms of GlyBP (0.16 – 0.2 mg/ml) in 25 mM potassium phosphate buffer, pH 7.4 were recorded at 25 °C in the near-UV length region (190–280 nm). At least ten reproducible spectra were collected for each preparation, averaged, and smoothed.

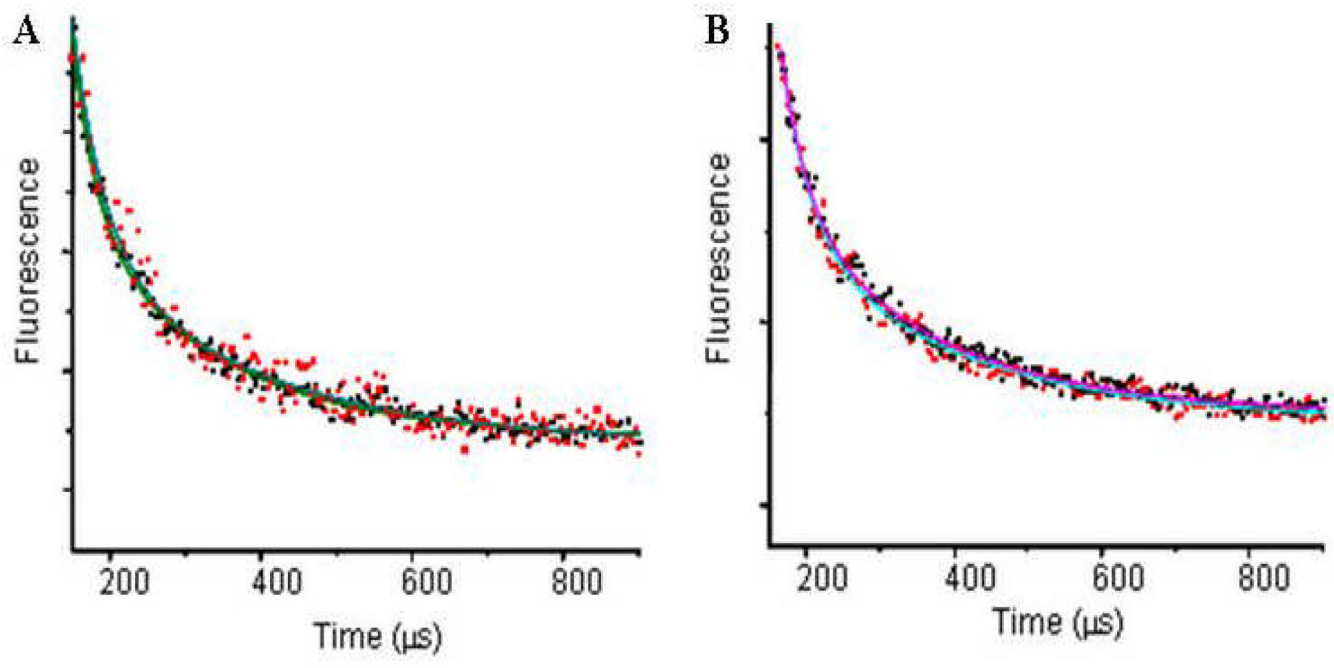

FIGURE 5.

Intersubunit spacing of tagged Cys-41 GlyBP determined by FRET. (A) The FRET lifetime as measured by the sensitized emission for the apo (red) and glycine bound (black) forms of GlyBP. (B) the FRET lifetime as measured by the sensitized emission for the apo (red) and glycine bound (black) forms of native GlyR expressed in insect cells.

Table 1

Calculated secondary structure from CD studies

Sample	Method	α_R	α_D	β-sheet	β-turn	Other	NRMSD
Aqueous GlyBP	CONTINLL	4%	9%	35%	13%	39%	0.028
Aqueous GlyBP	CDSSTR	2%	7%	37%	13%	40%	0.039
vesicular GlyBP	CONTINLL	5%	9%	33%	13%	40%	0.050
vesicular GlyBP	CDSSTR	3%	4%	41%	10%	40%	0.044

α_R and α_D are regular and distorted α-helix, respectively (34).

Reported values for % β -sheet are the sum of both its regular and distorted fractions.

Table 2

The fluorescence lifetimes and derived distances for GlyBP and full-length GlyR tagged with fluorescein (acceptor) and TTHA-Tb (Donor).

Sample	Ligand	Donor lifetime (μs)	Sensitized emission lifetime (μs)	Distance(Å)
GlyBP	Glycine	1392 ± 52	31 ± 4	31.9 ± 0.6
			198 ± 14	44.4 ± 0.7
GlyBP	Apo	1392 ± 49	44 ± 8	33.8 ± 1.0
			241 ± 52	46.2 ± 1.6
GlyR	Glycine	1654 ± 49	35 ± 5	31.9 ± 0.7
			225 ± 25	43.8 ± 1.0
GlyR	Apo	1680 ± 51	44 ± 4	33.1 ± 0.5
			252 ± 27	45.2 ± 1.1